Lewis Type Bombardment Ion Engine: d.c. and Pulsed Operation

H. J. KING* AND B. S. QUINTAL†
Ion Physics Corporation, Burlington, Mass.

Introduction: d.c. Operation

AN experimental program has been conducted to investigate the fundamentals of operation of a Lewis type[1] electron bombardment ion engine. This program has provided empirical evidence that either the arc or accelerating electrodes can limit the beam current from the engine, depending on operating conditions. It is found that, for an engine of a particular size, the thrust level, specific impulse, and propellant efficiency are interrelated and thus cannot all be chosen independently. It is shown that for a given specific impulse and maximum propellant efficiency, the thrust is directly related to engine size, being a linear function of beam area over the range investigated.

Limits of Engine Operation

The mechanism by which an ion beam is formed by this device has been discussed in the literature.[1-3] It is sufficient to say here, with reference to Fig. 1, that the propellant (i.e., mercury) fed into the arc chamber in vapor form is ionized by electron bombardment and fills the arc chamber with plasma. Ions are extracted from this plasma at the downstream end of the arc chamber and accelerated to the desired velocity by several kilovolts imposed between the pair of beam-forming electrodes. The magnetic field lines parallel to the axis of the engine confine the electrons in the arc chamber to circular orbits such as those found in a magnetron biased beyond cutoff, thus increasing the electron path length and, hence, the ionization efficiency.

Since it is desirable to maximize the beam current density, hence, the thrust for any engine, an experimental investigation was undertaken to determine how the various operating parameters interact to limit the output current. During all operating modes a small fraction of the ions extracted from the plasma will be collected on the downstream beam-forming electrode. This "intercepted current" directly determines the lifetime of the electrode and thus must be minimized, or at least limited to some small value, to give a best compromise of

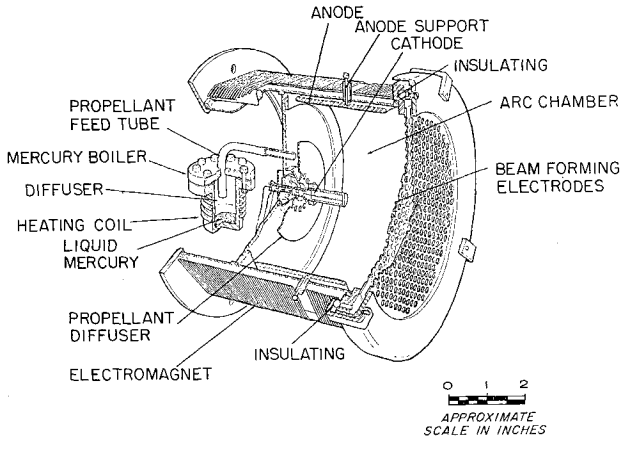

Fig. 1 Sectioned view of 13.7-cm diam ion engine.

Table 1 Engine parameters

Beam diameter (beam forming electrodes 50% opaque)	13.7 cm
Beam energy	3 to 6 kv
Accelerator electrode bias	−1 kv
Arc voltage[a]	50 v
Arc current Magnetic field	varied to produce the desired output current
Cathode temperature	970°C
Total power efficiencies[b]	75% to 85%
Pressure in vacuum tank during operation	3 to 5 × 10^{-6} Torr

[a] The arc voltage could, if desired, be varied as well to change the operating conditions. Arc instabilities are encountered at low propellant flow rates and arc voltages below 30 v (for an engine of this diameter). The percentage of Hg^{++} in the beam increases with arc voltage[4,5] making operation above ~60 v undesirable.

[b] Total power efficiency = $\left(\frac{\text{power in beam}}{\text{power in beam, arc, mag., cathode}}\right)$.

engine lifetime and output thrust. This boundary condition is important to the manner in which the experiment described below was conducted.

The engine shown in Fig. 1 was used throughout. The propellant feed system was calibrated to determine the propellant flow rate‡ as a function of boiler temperature. The engine parameters listed in Table 1 were maintained while the arc current was adjusted (by varying the magnetic field) to permit the maximum allowable current to be drawn from the engine at accelerating voltages of 3, 4, 5, and 6 kv.

The propellant flow rate was set at a series of discrete values between 50 and 450 mamp equivalent. For reasons just discussed, the maximum allowable output current was defined as that beam current at which the intercepted current on the accelerator electrode was less than 8 mamp.§ Results of this experiment are plotted in Fig. 2.

Several interesting conclusions can be drawn from Fig. 2. At low propellant feed rates the number density of neutral propellant atoms in the arc chamber is apparently so low that a true arc cannot form. The arc and beam currents are both independent of magnetic field above a small threshold field value. The intercepted current remains small.

At high feed rates the arc current can be driven to values greater than 10 amp by increasing the magnetic field. Such high values must be avoided during operation since the output beam associated with these arc currents exceeds the current handling capabilities of the beam-forming electrodes, thus causing large interception on the accelerator electrode. Limiting this interception to the forementioned 8 mamp, of necessity, limits the output for any given accelerating voltage as seen in Fig. 2. These limiting beam currents very closely follow the relation $I \propto V^{3/2}$.

Thus, two extremes of operation are observed: the propellant limited and accelerator limited modes. Operating points a few percent below the knee of the curves in Fig. 2 were normally chosen for extended runs. At this point the propellant efficiency goes through a broad maximum (maximum values to 90%), and very stable engine operation is observed. These results indicate that an increase in thrust from an engine of a given size (at a fixed I_{sp}) depends directly on increasing the current handling capabilities of the ion optical structures, either by using more complicated electrode geometries or by using a structure composed of more than two elements (i.e., an accel-decel arrangement).

Presented at the AIAA Electric Propulsion Conference, Colorado Springs, Colo., March 11–13, 1963; revision received September 3, 1963. The authors are grateful to S. V. Nablo and the Particle Physics Division of Ion Physics Corporation for their help in the successful completion of this project.

* Senior Physicist, Particle Physics Division; now at Hughes Research Laboratories, Malibu, Calif. Member AIAA.

† Engineer, Particle Physics Division. Member AIAA.

‡ Propellant flow rate in amperes is the current that would be carried by a given mass flow if each atom is singly ionized.

§ The value of 8 mamp maximum allowable intercepted current was chosen arbitrarily. This value corresponds to ~2% of the beam current from the engine at I_{sp} = 8000 sec and represents a point where the accelerator electrode is not seriously damaged during several days of data taking. A lower value would most certainly be chosen in the design of a flight model engine.

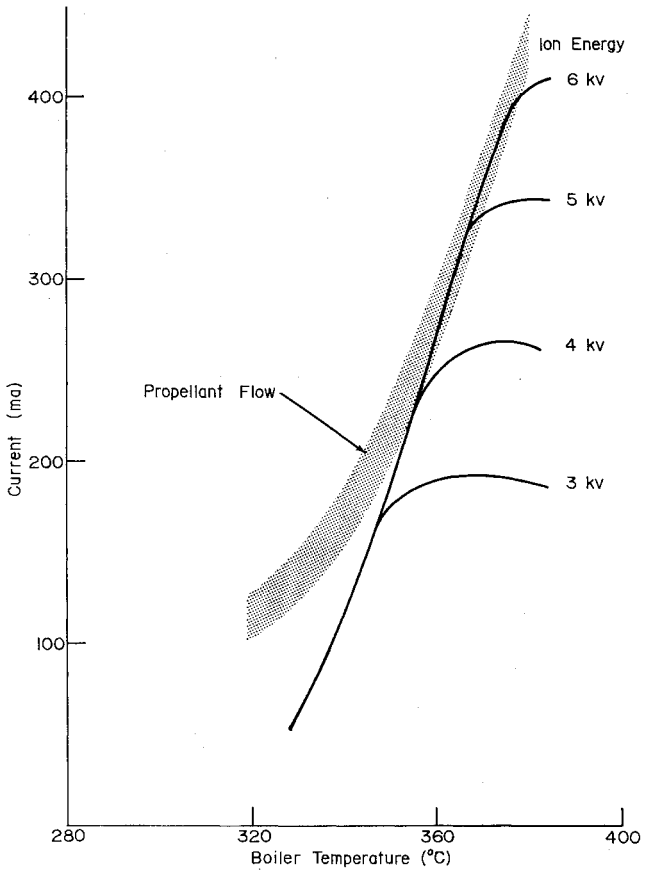

Fig. 2 Output current vs propellant flow rate (boiler temperature) measured during tests.

Scaling Relations

Engines producing beams varying in diameter from 4.5 to 13.7 cm have been studied. All had similar operating characteristics to the forementioned and produced the same limiting current densities at approximately 2% interception. It was found that the smaller the engine the lower the arc voltage required for stable operation. Small engines, however, required a larger value of [arc current/beam current], thus keeping the arc power required to produce a given beam current approximately constant. The linear relation between thrust (at a given I_{sp}) and beam area permits design of an engine to meet specific requirements. The power efficiencies should be almost independent of engine size assuming the cathode and magnet are tailored to the specific engine under consideration. Structural problems associated with very large or very small engines may well limit the useful range over which the forementioned relation may be applied. It was also found during the course of the studies that higher propellant efficiencies were attained with the largest engine studied (13.7-cm diam.). A clearcut variation of propellant efficiency with size was not, however, established, and the forementioned result may well have been either fortuitous or a result of the fact that the operators had a better "feel" for the performance of this engine because of its extensive use during the tests.

Pulsed Operation

The pulsed operation of a Lewis type[1] ion engine was studied in an attempt to determine the feasibility of developing such a device for precise thrust vectoring or positioning of space vehicles. The engine used was very similar in structure to that shown in Fig. 1, except that the anode diameter was 4.5 cm and that a gas feed system was used. Argon and xenon were used as propellants. These studies proved that beam-current pulses could be produced by the simple expedient of pulsing the arc voltage with the cathode, magnet, propellant

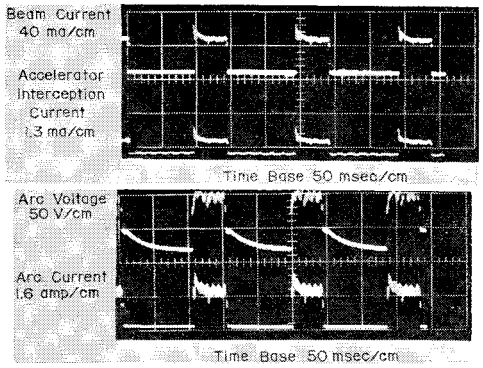

Fig. 3 Pulse shapes observed during engine operation.

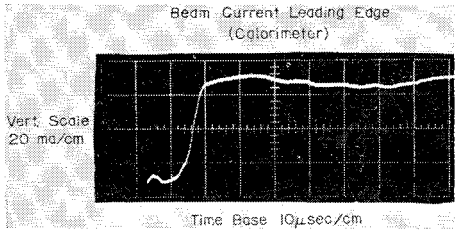

Fig. 4 Leading edge of beam pulse measured at calorimeter 30 cm from engine.

flow, and high voltage in the "operate" mode. These latter parameters may be adjusted to their correct values while the arc is off and, thus, will not affect the transient response of the thrust pulse.

D.c. beam currents of 40 mamp of xenon were established at 5 kv. Operation was then changed to the pulsed mode by pulsing the voltage on the grids of the series tubes in the arc supply with a pair of time delay relays. Pulse lengths and repetition rates were adjustable from 10 msec to 3 sec. The current and voltage pulses from the arc supply could be monitored on an oscilloscope (with no acceleration voltage on the engine). The intercepted current on the acceleration electrode, as well as the current pulse reaching the beam collector 30 cm downstream, could be monitored during engine operation. Oscilloscope traces of these measurements are shown in Fig. 3 and Fig. 4. Oscillations are evident on the leading and mid-portion of the pulse. These are inherent in the power supply pulsing mechanism rather than the engine.

The d.c. operating point is reproduced to within the accuracy of the measurements during pulsed operation. No increase in interception was attributed to pulsed operation. In all, 250,000 pulses were produced with no apparent damage to the accelerator electrode.

The only appreciable time delay in producing a thrust pulse starting with all systems in the "off" position is the thermal time constant of the cathode. Investigation of the effects that accelerated cathode warmup have on cathode lifetime has not been completed, so it is presently not possible to estimate fully the capabilities of such a bombardment thrustor in attitude control application. Trends toward increased cathode efficiencies and reliabilities give promise that it may soon be feasible to run the cathode at operating temperature for the useful life of the system, thus reducing the total time to ready the engine for a thrust pulse to a matter of milliseconds.

References

[1] Kaufman, H. R., "An ion rocket with an electron bombardment ion source," NASA-TN-D-585 (1961).

[2] Reader, P. D., "Investigation of a 10 cm diameter electron bombardment ion rocket," NASA-TN-D-1163 (January 1962).

[3] Kaufman, H. R., "The electron bombardment ion rocket," *AFOSR Symposium on Advanced Propulsion Concepts*, (Cincinnati, Ohio, October 1962).

[4] Milder, N. L., "Comparative measurements of singly and

doubly ionized mercury produced by electron bombardment ion engine," NASA-TN-D-1219 (July 1962).

[5] "Low current density ion engine development," Final TR Contract NAS8-1684, Ion Physics Corp., Burlington, Mass. (January 1963).

Effect of Transient Creep on the Collapse Time of Cylinders and Cones under External Pressure

E. Z. Stowell* and E. M. Briggs†
Southwest Research Institute, San Antonio, Texas

Nomenclature

A = cross-sectional area, in.^{2}
E = elastic tensile modulus, ksi
h = thickness of solid wall, or distance between facings in sandwich wall, in.
P = applied load, lb
s = material constant, hr^{-1}-deg^{-1}-°K
ΔH = material constant, cal-mol^{-1}
σ_0 = material constant, ksi
T = temperature, °K
M = temperature constant = $2sTe^{-\Delta H/RT}$ hr^{-1}
t = time, hr
α = nondimensional material constant for transient creep defined in text as $E_I/(E_I + E_{II})$
β = nondimensional material constant for transient creep defined in text as M_I/M_{II}
w = deflection, in.
ϵ = strain
σ = stress, ksi
$\bar{\sigma}$ = mean stress = P/A, ksi
σ_{cr} = elastic critical stress, ksi
τ = time constant, hr

Subscript

I,II = referring to different parts of the material
1,2 = referring to different sandwich facings

Introduction

MEASUREMENTS of the creep collapse times of long cylindrical shells under external pressure[1] and of finite cylindrical shells and cones[2,3] have been reported in the literature.

On the assumption that creep collapse occurs as a result of growth of the initial imperfections with time, a theory using steady-state creep has been developed, and a formula for the time to collapse has been derived. Comparisons of these theoretical results with experiment have been made[1–4] which showed the basic soundness of the theoretical foundation. In Ref. 4, for example, it was found that columns and cylindrical shells, with their widely different initial imperfections, could be handled by the same formula and plotted on the same chart.

The accuracy of the prediction of collapse time, however, in some cases left something to be desired. It was felt that one of the principal reasons for this lack of accuracy was the neglect of the transient component of creep. The theory assumed a constant creep rate throughout, whereas it was inevitable that the creep rates would be much higher than this constant value for a time following the application of external pressure. The question arose as to how much the time to collapse would be affected by the inclusion of the transient component of creep.

Received June 7, 1963; revision received September 25, 1963. This research was supported by the U. S. Air Force under Contract AF 33(657)-8125, monitored by the Thermomechanics Research Laboratory, Aeronautical Research Laboratories, Wright-Patterson Air Force Base, Ohio.

* Institute Scientist.
† Assistant Research Engineer.

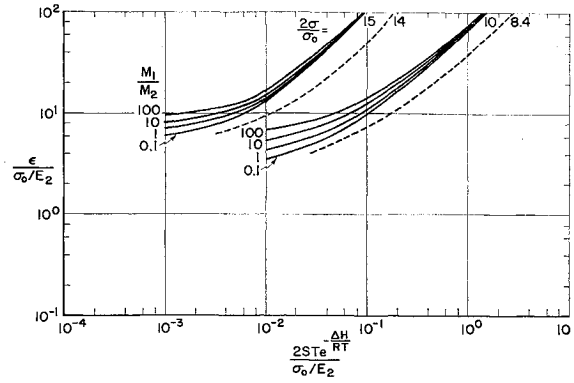

Fig. 1 Transient creep of 3003-H14 aluminum alloy shown as dashed curves superimposed on Fig. 1a of Ref. 5.

Fortunately, the mechanism for handling this problem was available.[5] Although three constants are sufficient to determine completely the steady-state creep, two additional constants, making five in all, are required to include the transient component. This generalization was employed in the attempt to improve the accuracy of collapse time predictions.

Analysis

In Ref. 5, a phenomenological theory was developed to account for the phenomena of transient creep. The distinguishing characteristic of this theory is that after a time the creep becomes steady, and so the theory includes within itself both the transient and the steady creep. The theory shows that by knowledge of five constants, it is possible to describe the entire family of creep curves for any material up to the beginning of tertiary creep. Three of the constants are those associated with the steady state of creep, whereas the remaining two serve to specify the transient state of creep. In Ref. 5, it was shown that the families of creep curves for four different materials (pure aluminum, gamma iron, lead, and 7075-T6 aluminum alloy) could be described completely by these five constants.

The theory assumes that any given material is split into two parts, each of which is itself viscoelastic with its own elasticity and its own viscosity. It is the interaction of these two parts which produces the transient creep. As time progresses, the interaction between the parts becomes of less and less importance, until the interaction substantially ceases, and the material then creeps at a steady rate.

The notation is the same as that used for steady state creep, with the addition of subscripts I and II for the two parts of

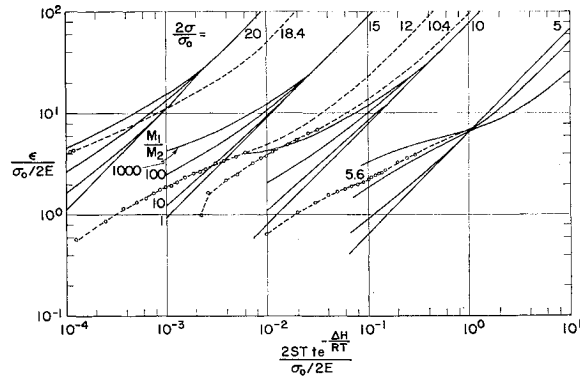

Fig. 2 Transient creep of 6061-T6 aluminum alloy shown as dashed curves superimposed on Fig. 1b of Ref. 5.